Chlordecone-contaminated epilithic biofilms show increased adsorption capacities

Cédric Hubas, Dominique Monti, Jean-Michel Mortillaro, Sylvie Augagneur, Anne Carbon, Robert Duran, Solange Karama, Tarik Meziane, Patrick Pardon, Théo Risser, et al.

Chlordecone-contaminated epilithic biofilms show increased adsorption capacities

Cédric Hubas[1*], Dominique Monti[2,4], Jean-Michel Mortillaro[3,8], Sylvie Augagneur[6,7], Anne Carbon[5], Robert Duran[5], Solange Karama[5], Tarik Meziane[3], Patrick Pardon[6,7], Théo Risser[5], Nathalie Tapie[6,7], Najet Thiney[3], Hélène Budzinski[6,7], Béatrice Lauga[5]

*corresponding author : Tel.: +33-298509933, E-mail: cedric.hubas@mnhn.fr

1- Muséum National d'Histoire Naturelle, Laboratoire Biologie des Organismes et Ecosystème Aquatiques (UMR 8067 BOREA), Sorbonne Université, CNRS, IRD, Université de Caen Normandie, Université des Antilles; Station Marine de Concarneau, Quai de la croix, 29900 Concarneau, France

2- Université des Antilles, Laboratoire Biologie des Organismes et Ecosystème Aquatiques (UMR 8067 BOREA), Muséum National d'Histoire Naturelle, Sorbonne Université, CNRS, IRD, Université de Caen Normandie; Campus de Fouillole, 97110 Pointe-à-Pitre, France

3- Muséum National d'Histoire Naturelle, Laboratoire Biologie des Organismes et Ecosystème Aquatiques (UMR 8067 BOREA), Sorbonne Université, CNRS, IRD, Université de Caen Normandie, Université des Antilles; 61 rue Buffon, 75005 Paris, France

4- Université des Antilles, Institut de Systématique, Evolution, Biodiversité (UMR 7205 ISYEB), Muséum National d'Histoire Naturelle, CNRS, Sorbonne Université, EPHE; Campus de Fouillole, 97110 Pointe-à-Pitre, France

5- Universite de Pau et des Pays de l'Adour, E2S UPPA, CNRS, IPREM ; Pau, France

6- Université de Bordeaux, Environnements et Paléoenvironnements Océaniques et Continentaux (EPOC - UMR 5805 CNRS), Equipe LPTC; 33405, Talence, France

7- CNRS, Environnements et Paléoenvironnements Océaniques et Continentaux (EPOC - UMR 5805 CNRS), Equipe LPTC; 33405, Talence, France

8- ISEM, Univ Montpellier, CNRS, IRD, CIRAD, Montpellier, France

Graphical abstract

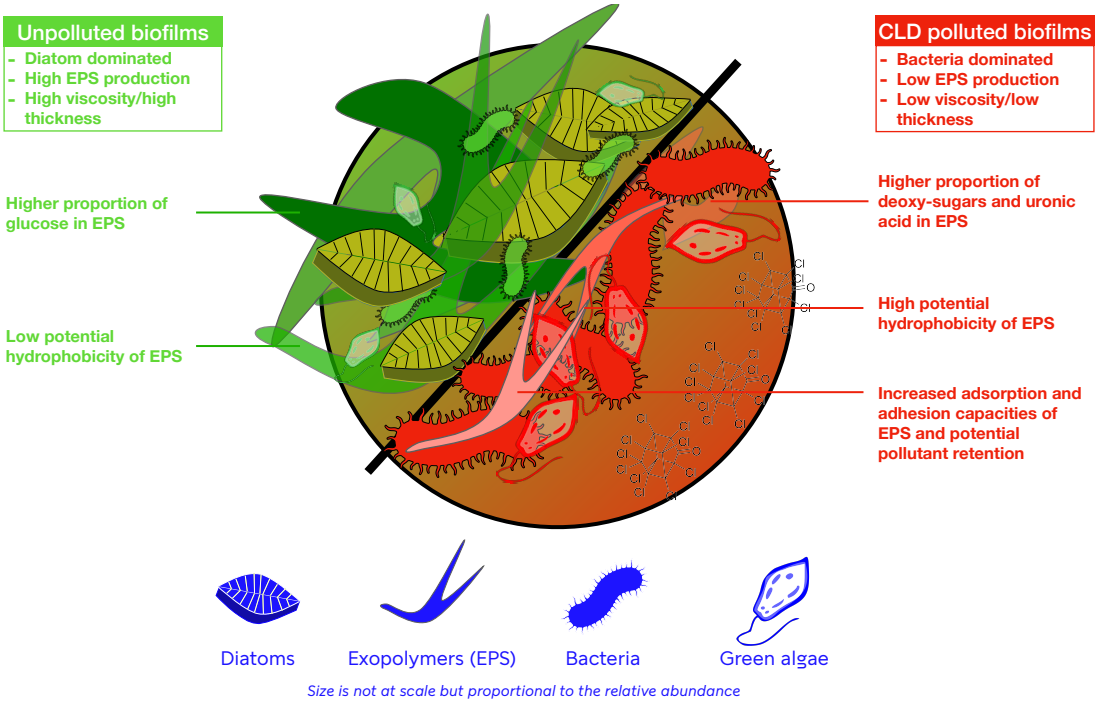

Abstract

The rivers of Guadeloupe and Martinique (French West Indies) show high levels of chlordecone (CLD) contamination. This persistent moleculehas a dramatic impact on both aquatic ecosystems and human health. In these rivers, epilithic biofilms are the main endogenous primary producers and represent a central food source for fish and crustaceans. Recently, their viscoelastic properties have been shown to be effective in bio-assessing pollution in tropical environments. As these properties are closely related to the biochemical composition of the biofilms, biochemical (fatty acids, pigments, extracellular polymeric substances (EPS) monosaccharides) and molecular markers (T-RFLP fingerprints of bacteria, archaea and eukaryotes) were investigated. Strong links between CLD pollution and both biofilm biochemistry and microbial community composition were found. In particular, high levels of CLD were linked with modified exo-polysaccharides corresponding to carbohydrates with enhanced adsorption and adhesion properties. The observed change probably resulted from a preferential interaction between CLD and sugars and/or a differential microbial secretion of EPS in response to the pollutant. These changes were expected to impact viscoelastic properties of epilithic biofilms highlighting the effect of CLD pollution on biofilm EPS matrix. They also suggested that microorganisms implement a CLD scavenging strategy, providing new insights on the role of EPS in the adaptation of microorganisms to CLD-polluted environments.

Keywords: epilithic biofilms; chlordecone; extracellular polymeric substances; microbial communities; T-RFLP; fatty acids ; monosaccharides, lipophilic pigments ; Caribbean

Introduction

At the beginning of the 2000's, high chlordecone ($C_{10}Cl_{10}O$; CAS number 143-50-0 | Kepone®) contamination levels have been reported in Guadeloupe and Martinique (French West Indies) rivers. Though chlordecone (CLD) usage was banned in the 1990's, and despite reported potential degradability similar to other organochlorine (OC) pesticides (Dolfing et al., 2012), CLD, was found to be highly present in soils, reaching 35 $mg \cdot kg^{-1}$ ten years after the last agricultural spreading (Martin-laurent et al., 2013). The widespread use of CLD for the intensive cropping of bananas had caused ecological as well as a public-health disaster in the French West Indies. Indeed, despite being reported as a possible human carcinogen in late 1970's (Reuber, 1978), CLD was yet used for about 20 years and afterwards identified as the main cause of the increased prevalence of prostate cancer in Martinique (Belpomme and Irigaray, 2011; Multigner et al., 2010).

To date most studies have focused on microbial ecology of CLD-contaminated soil (andosols, ferralsols, and nitisols), evidencing that CLD changed soil microbial communities according to the contamination level and physical-chemical soil characteristics (Mercier et al., 2013; Merlin, 2015). Though evidences in soil microcosms confirmed the existence of potentially CLD-respiring or -fermenting microorganisms, CLD-degradation metabolites have yet to be detected in soils (Fernández-Bayo et al., 2013). Also, the reported CLD mineralisation rates are well below those necessary to remove completely the CLD (Fernández-Bayo et al., 2013). In contrast, microbial communities of French West Indies rivers have been seldom studied so far despite the recognized contamination, at varying levels, of numerous aquatic systems (Crabit et al., 2016). This is surprising since during the massive CLD-contamination of the Saint James River (Virginia, USA) in the 1970's (Huggett, 1989) the disruptive effects of CLD on survival and growth of a significant fraction of bacteria inhabiting the water column and the sediment were demonstrated (Orndorff and Colwell, 1980). In Guadeloupe, due to turbulent flows and high-water velocity, autochthonous river primary production is mainly supported by epilithic biofilms growing on riverbed stones. These biofilms are one of the few food sources that are accessible to higher trophic levels in this habitat (Coat et al., 2009; Lefrançois et al., 2011). Recent studies have shown a very low level of essential fatty acids (eicosapentaenoic acid, EPA) in aquatic species living in the rivers of Guadeloupe, and as this molecule is contained in the epilithic biofilm consumed by these species, this suggests that dietary EPA may be a limiting factor for growth or survival (Frotté et al., 2021).

Biofilms are complex and highly organized assemblages characterized by a great diversity of microorganisms (algae, fungi, protozoa, bacteria and archaea) embedded in a matrix of extracellular polymeric substances (EPS) produced by the microorganisms . The EPS are ubiquitous component of epilithic biofilms primarily composed of high molecular weight polymers, such as carbohydrates and proteins, containing charged functional groups (Decho, 2000; Decho et al., 2010). These functional groups provide binding sites that serve as natural adsorptive and adhesive supports for charged particles/molecules, including pollutants (Bhaskar and Bhosle, 2006), then available for bioaccumulation in aquatic food webs (Decho, 2000; Decho et al., 2010).

More recently, the relationships between viscoelastic properties of epilithic biofilms and their EPS production were pointed out in relation to CLD pollution (Monti et al., 2020). However, the CLD effect on EPS chemistry was not addressed.

In the present study, we characterized the EPS composition of epilithic biofilms in relation to CLD pollution combining a set of chemotaxonomic biomarkers (fatty acids, lipophilic pigments), EPS biochemical markers (monosaccharides), as well as molecular fingerprints of prokaryotic and eukaryotic communities based on 16S- 18S rRNA genes, respectively. The main objective of the study was to examine changes in the EPS matrix as well as in the microbial composition of the biofilm in response to CLD pollution to better understand the changes previously observed in the viscoelastic properties of epilithic biofilms.

Materials and methods

Sampling site and experimental design: Biofilms were obtained from 6 rivers in February 2013. Rivers were located in the western-half of Guadeloupe (i.e. Basse-Terre island, figure 1) and were chosen according to their content in CLD and their ability to contain pristine waters upstream from the banana plantations and contaminated waters downstream from the banana fields (i.e. one sampling site above banana fields and one sampling site below for each river: 12 sampling sites in total). All the rivers belong to the same hydroecoregion, a homogenous zone regarding geology, climate and landscape. Additional information about the sampling sites is available in Monti et al. (2020, i.e. first sampling campaign, February 2013). Biofilms were obtained by immersing glass slides (76x26 mm) which were then collected in triplicates 7, 14 and 21 days after immersion (hereafter named T07, T14 and T21) as described by these authors. Glass slides were carefully wrapped in foil after sampling and kept cold until return to laboratory. They were then stored at –20°C until analysis. In each river, water samples were taken (100 mL) to measure the CLD concentration, at each sampling date.

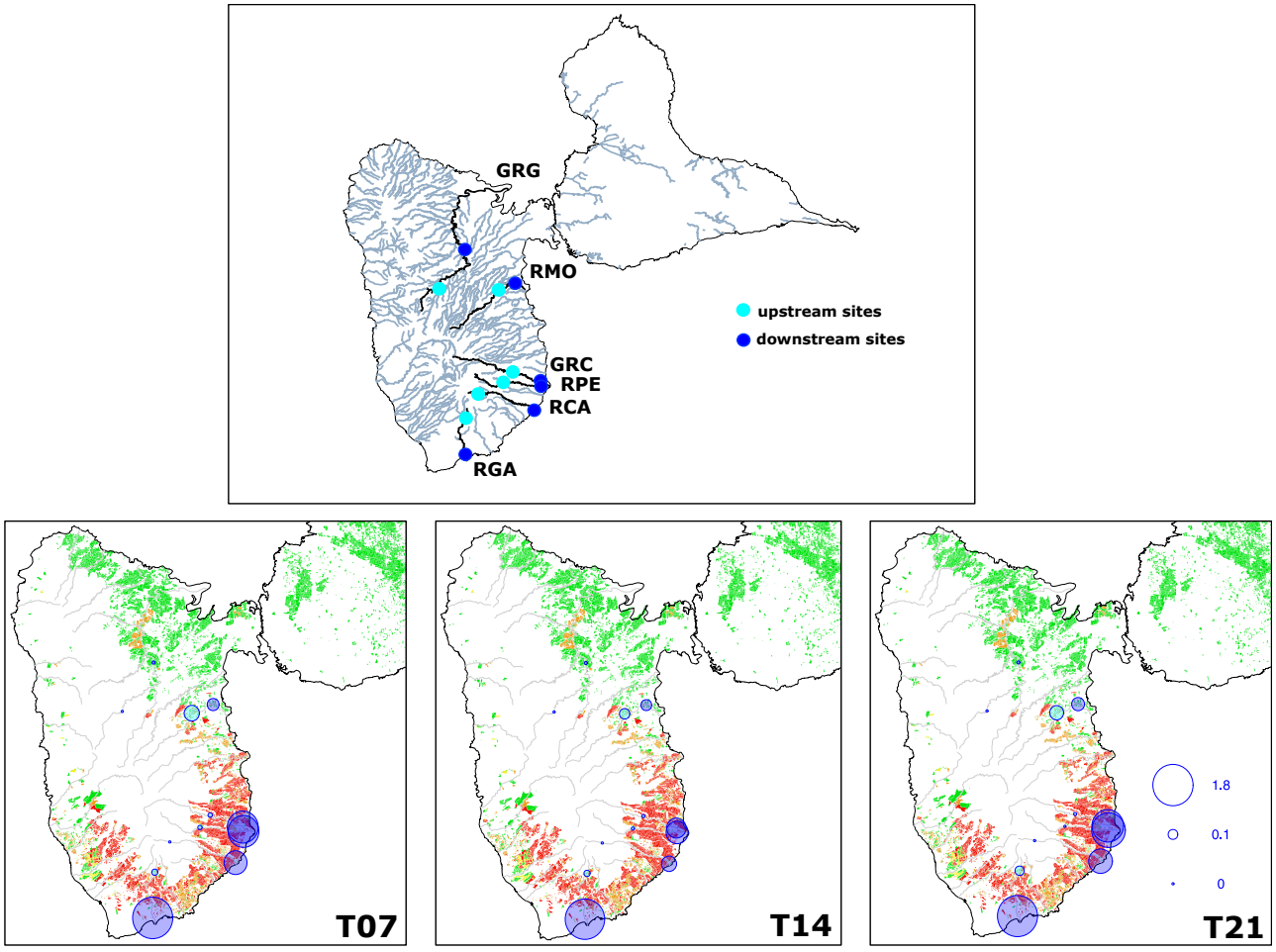

Figure 1: Description of the sampling site. Upper panel: Localisation of the upstream (light-blue) and downstream (darkblue) sampling sites in 6 different rivers. Grande rivière à Goyaves River: GRG, Moustique River: RMO, Grande rivière de Capesterre River: GRC, Pérou River: RPE, Carbet River: RCA, Grande Anse River: RGA. Bottom panel : vector based mapping of the potential CLD pollution according to the French DAAF (Direction de l'Alimentation, de l'Agriculture et de la Forêt de Guadeloupe) regulation (calculated from satellite imaging and archives data of banana plantations). Red = severe, orange = high, yellow = low, Green = minor. The size of the light-blue and dark-blue circles is proportional to the CLD concentrations (in µg·L−1) measured during the February 2013 campaign in river waters. From left to right : Levels of CLD pollution in river waters 7, 14 and 21 days after immersion of the glass slides. (For interpretation of the references to color in this figure legend, the reader is referred to the web version of this article.)

Chlordecone extraction and analysis: Water samples collected into glass bottles were stored at -20°C until analysis. They were thawed before extraction, and processed without filtration step because of the low quantity of suspended matter presents in the samples. Water samples of 100 mL were spiked with internal standard solution (chlordecone ^{13}C) and were then extracted with 10 mL of dichloromethane three times. These extracts were dried on sodium sulphate (Na_2SO_4) and then evaporated under a gentle flow of nitrogen. The final extract was transferred into 100 µL of acetonitrile for injection. The extracts were analyzed by HPLC-ESI-MS-MS (UPLC-Quattro premier Waters). Separation was achieved using a BEH-C18 column (50 mm x 2.1 mm; 1.7 µm) at

a temperature of 35°C. Acetonitrile and water (ultrapure deionized water) were used as the mobile phases. The injection was carried out using 5 µL of sample and the flow rate was 0.6 mL.min^{-1}. The gradient composition of the mobile phase started with 0% of acetonitrile and increased up to 100% in 3 min. This composition was held for 0.5 min and then decreased down to 0% in 0.5 min and was held at 0% until the end of the analysis. The spectrometer was operated with a negative electrospray ion source (ESI) and multiple reaction monitoring mode (MRM) using nitrogen as the collision gaz. Quantification were made with internal standard. Analytical method was validated in terms of calibration linearity, specificity, extraction recoveries (93 ± 8%), and limits of quantifications (2 pg injected or 1 ng·L^{-1}). For each series of analysis, blank experiments (complete procedure but without matrix) were performed. Recoveries of three samples of fortified mineral water (50 ng·L^{-1}) were evaluated for water analysis (from 90 to 105%). Control calibrating standards (0.1 à 100 ng·g^{-1}) were also injected every 15 samples and analytical blanks were performed. All solvents for chemicals analysis, dichloromethane (DCM) and acetonitrile (ACN) (HPLC reagent grade, Scharlau) were purchased from ICS (Belin Beliet, France). Analytical standards of CLD were purchased from LGC Standards (Molsheim, France)

Fatty acid composition: Fatty Acids (FA) were extracted following the method of Bligh and Dyer (1959). Total lipids were extracted by scraping the glass slides with a pre-combusted GF/F filter saturated with 2 mL of methanol (MeOH). Lipids were extracted with a 20 min ultrasonication (sonication bath, 80 kHz, Fisherbrand™) in a mixture of distilled water, chloroform and methanol in ratio 1:1:2 (v:v:v, in mL). An internal standard (23:0) was added to every sample for quantification purpose (0.5 mg·mL^{-1}). Lipids were concentrated under N_2 flux, and saponified, in order to separate FA, with a mixture of NaOH (2 mol·L^{-1}) and methanol (1:2, v:v, in mL) at 90°C during 90 min. Saponification was stopped with 400 µL hydrochloric acid. Samples were then incubated with BF3-methanol at 90°C during 10 min to transform free FA into fatty acids methyl esters (FAME), which were isolated and kept frozen in chloroform. Just before analysis, samples were dried under N_2 flux and transferred to hexane. One µL of the mixture was injected in a gas chromatograph (GC, Varian CP-3800 equipped with flame ionization detector), which allowed separation and quantification of FAME. Separation was performed with a Supelco® OMEGAWAX 320 column (30 m × 0.32 mm i.d., 0.25 µm film thickness) with He as carrier gas. The following temperature program was used: 60 °C for 1 min, then raise to 150 °C at 40 °C·min^{-1} (held 3 min), then raise to 240 °C at 3 °C·min^{-1} (held 7 min) at 1 mL·min^{-1}. FAME Peaks were identified by comparison of the retention time with analytical standards. Additional identification of the samples was performed using a gas chromatograph coupled to mass spectrometer (GC-MS, Varian 450GC with Varian 220-MS). Compounds annotation was performed by comparing mass spectra with NIST

2017 library. Fatty acids were quantified using the FID detector and the internal standard. Corresponding fatty acids are designated as X:Yn-Z, where X is the number of carbons, Y the number of double bonds and Z the position of the ultimate double bond from the terminal methyl.

Pigment composition: Lipophilic pigments were extracted by scraping the glass slides with a GF/F filter saturated with 2mL of MeOH. Filters were placed in a sterile tube and crushed in 2 mL of 95 % cold buffered MeOH (2 % ammonium acetate) for 4h at 4°C, in the dark. Samples were sonicated (37 kHz) for 30 s prior to extraction. Extracts were then filtered (0.2 µm) immediately before High Performance Liquid Chromatography (HPLC) analysis according to Brotas and Plante-Cuny (2003). Pigment extracts were analysed using an Agilent 1260 Infinity HPLC composed of a quaternary pump (VL 400bar), a UV-VIS photodiode array detector (DAD 1260 VL, 190 to 950 nm), and a 100 µL sample manual injection loop (overfilled with 250 µL). Chromatographic separation was carried out using a C18 column for reverse phase chromatography (Supelcosil, 25 cm long, 4.6 mm inner diameter). The solvents used were A: 0.5 M ammonium acetate in methanol and water (85:15, v:v), B: acetonitrile and water (90:10, v:v), and C: 100 % ethyl acetate with a flow rate of 0.5 $mL.min^{-1}$. Identification and calibration of the HPLC peaks was performed with chlorophyll *a*, astaxanthin, β-carotene, chlorophyll *c*, fucoxanthin standards. Pigments were identified by their absorption spectra and relative retention times. Quantification was performed by repeated injections of standards over a range of dilutions to determine the relationship between peak area and standard concentrations. The relative abundance of each pigment (%) was calculated from their respective concentration ($\mu g \cdot cm^{-2}$).

Monosaccharide composition of exopolymers: Colloidal and bound exopolymers (EPS) of the biofilms were extracted by rotating the glass slides in a mixture of distilled water and ion-exchange resin (Dowex Marathon C, sodium, Sigma) for 1.5 h at 4°C. Glass slides were placed in 50 ml tubes filled with the mixture so that they were immersed during the agitation procedure. The exopolymer solution was then retrieved and freeze-dried. Monosaccharide composition was determined using gas chromatography (GC), following Passarelli et al. (2015). EPS were hydrolysed in 2 $mol \cdot L^{-1}$ HCl, and heated 4 h at 90°C to release individual monosaccharides prior their derivatization (silylation), which was performed with a mixture of BSTFA:TMCS (N,O-bis(trimethylsilyl)trifluoroacetamide and trimethylchlorosilane, 100:1, Sigma) and pyridine (1:1, v:v), for 2 h at room temperature. After the silylation, 1 µL of the sample was injected in GC (GC, Varian CP-3800 equipped with flame ionization detector), which allowed separation and relative quantification of monosaccharides. Separation was performed with an Agilent Technologies VF-1701ms column (30 m × 0.32 mm i.d., 0.25 µm film thickness) with He as carrier gas. The

following temperature program was used: start at 150 °C, raise to 200 °C at 7 °C·min^{-1} (held 5 min). Injector temperature was set at 250 °C. Peaks of monosaccharides were identified by comparison of the retention time with analytical standards (rhamnose, fucose, xylose, mannose, galactose, glucose, scyllo- and myo-inositol, galacturonic and glucuronic acid), which had been prepared (silylation and injection only) as samples.

DNA extraction and T-RFLP analysis: For each sampling point epilithic biofilms were removed from three slides with a sterile toothbrush in 50 mL of sterile ultrapure water. Collected water was then filtered onto a 0.22 µm sterile cellulose nitrate membrane filter (Sartorius, Goettingen, Germany) and filters were stored at -80°C until DNA extraction.

The Power Water DNA Isolation Kit (Mo Bio Laboratories, Solana Beach, CA, USA) was used to extract total biofilm DNA according to the manufacturer's instructions. The quantity and quality of the DNA extracts were checked by 1 % agarose gel electrophoresis, ethidium bromide staining and UV-translumination. The Bacteria universal primers 357F (5'-CCTACGGGAGGCAGCAG-3') (Teske et al., 1996) and 926R (5'-CCGTCAATTCMTTTRAGT-3') (Lane, 1991) and the Archaea universal primers 349F (5'-GYGCASCAGKCGMGAAW-3') and 806R (5'-GGACTACNNGGGTATCTAAT-3') (Takai and Horihoshi, 2000) were used to amplify the 16S rRNA gene. The Eukarya primers targeting 18S rRNA genes were HEX uk-1A-F (5'-CTGGTTGATCCTGCCAG-3') (Sogin and Gunderson, 1987) and Euk-516-GC-R (5'-ACC AGA CTT GCC CTC C-3') (Amann et al., 1990). Forward primers were 5' labelled with carboxyfluorescein (FAM) for prokaryotes and with hexa-chloro-fluorescein-phosphoramidite (HEX) for eukaryotes. An initial denaturation (98°C for 30 s) followed by 30 cycles of denaturation (98°C for 10 s), annealing (58°C for 30 s), and extension (72°C for 30 s) and a terminal extension at 72°C for 10 min were used for PCR reactions. The reaction mixture was as followed: 0.5 µM of each primer, 12.5 µL of AmpliTaq Gold® 360 Master Mix (Applied Biosystems, Carlsbad, CA, US) and 1 µL of DNA template. Sterile distilled water was added up to 25 µL of final volume. PCR products were visualized on agarose gel and then purified with the PCR purification kit (GE Healthcare, Velizy-Villacoublay, France). After purification the amplicons (100 ng per sample) were digested by 3 U of AluI restriction enzyme (New England Biolabs) for 3 h at 37°C. The digested products (1 µL) were mixed with 8.75 µL of deionized formamide and 0.25 µL of the Genescan ROX 500 size standard (Applied Biosystems Carlsbad, CA, US). Fluorescently labelled fragments were separated with ABI PRISM 3130xl Genetic Analyzer (Applied Biosystems, Carlsbad, CA, US). Raw T-RFLP profiles obtained through GENEMAPPER software (version 1.4, Applied Biosystems, Carlsbad, CA, US) were normalized and analysed using T-REX to produce the final terminal fragments (T-RFs) data matrix (Culman et al., 2009). Only T-RFs with size ranging from

35 bp to 500 bp and with height > 30 fluorescence units were considered for analysis as described in Volant et al. (2014).

Statistical analyses: All statistical analyses were performed using R studio Version 1.2.5033 and packages ggplot2 (Wickham, 2016), scales (Wickham and Seidel, 2020), corrplot (Wei and Simko, 2021) and cowplot (Wilke, 2019) for data processing and visualisation. Raw data file together with in-house R script for data processing, univariate and multivariate statistics as well as figures are available at github repository: https://github.com/Hubas-prog/CLD-Biofilm. All maps were drawn using the Open Source Geographic Information System QGIS 2.10.1. For univariate comparisons, normality and homogeneity of variance were systematically checked and statistical tests chosen accordingly.

For multivariate comparisons, permutational multivariate analysis of variance (Permanova) was calculated using the Bray-Curtis dissimilarity index and 999 permutations. Homogeneity of multivariate dispersion was systematically checked prior to Permanova.

Multiple Factor Analyses (MFA) were performed according to Escofier and Pagès (1994) using the package ade4 in order to find common structures in several groups of variables defined on the same set of individuals. MFA analysis is a specific case of principal component analysis (PCA) applied to a table for which several groups of variables can be identified and for which each column of group *i* is weighted by the inverse of the first PCA eigenvalue of group *i*. . The biochemical markers were all measured on the same set of statistical individuals (i.e., on the same glass slides). The same applies to the molecular markers. However, it was not possible to perform a unique MFA using all these markers together as molecular and biochemical markers were not measured on the same glass slides. One MFA was thus performed using the three groups of biochemical markers (fatty acids, lipophilic pigments and EPS monosaccharides) and another MFA was performed using the three groups of molecular markers (targeting Bacteria, Archaea and Eukaryotes)

Additionally, in order to explore the weight of a given factor, we performed a supervised Between Class Analysis (BCA) by decomposing the total inertia of the MFA dataset according to a given instrumental variable (i.e., CLD pollution context). The final result is a supervised MFA called BC-MFA. Percentage of total inertia explained by the instrumental variable was calculated and a Monte Carlo test was performed to test the significance of the BC-MFA ordination. The above-mentioned statistical procedure was previously detailed elsewhere (Lavergne et al., 2017) and can be downloaded at the following repository: https://github.com/Hubas-prog/BC-MFA (doi: 10.5281/zenodo.4603552). A threshold based on the square cosine of the coordinates of the variables was applied for highlighting the most discriminating variables of the BC-MFA.

Chlordecone effect was also tested by fitting the CLD concentrations to the first and second axis of the MFA ordination.

Results

Chlordecone contamination in river water:

The water in upstream sites was significantly less impacted (or not affected at all) by CLD than in downstream sites (Wilcoxon signed rank test, p=0.001) with an average of 0.05 ± 0.07 and 0.68 ± 0.61 $\mu g \cdot L^{-1}$, respectively (Fig. 1). The only exception being the RMO River, where the upstream site had similar CLD concentrations as the downstream site (Wilcoxon signed rank test, p=0.5). CLD pollution changed significantly over time: on average, CLD concentrations significantly decreased from T07 to T14 (paired *t* test, df=5, p= 0.028),then significantly increased from T14 to T21 (paired *t* test, df=5, p= 0.028)

As pointed out previously by Monti et al. (2020), CLD measurements revealed three pollution contexts: a very limited or unpolluted context (UnP: between undetectable to 0.1 µg/L), a medium polluted context where values are comparable with those currently observed in the rivers of Guadeloupe and Martinique (Med: from 0.1 to 1 $\mu g \cdot L^{-1}$), and extreme situations (Ext: > 1 $\mu g \cdot L^{-1}$ and up to 2.76 $\mu g \cdot L^{-1}$), downstream from the banana plantations. Focusing on downstream sites, CLD concentrations were thus further categorized according to Monti et al., (2020) as unpolluted (UnP), moderately polluted (Med) and extremely polluted (Ext). The BC-MFA were performed using these categories as an instrumental variable.

Biochemical fingerprinting of epilithic biofilms:

Fatty acid composition: On average, the highest concentrations of total, saturated and mono-unsaturated FA were found in the upstream section of the RMO River (total: 15.18 ± 14.03 $\mu g \cdot cm^{-2}$, saturated FAs: 7.64 ± 7.48 $\mu g \cdot cm^{-2}$, mono-unsaturated FA: 4.40 ± 4.61 $\mu g \cdot cm^{-2}$) and the lowest in the upstream section of the RPE River (total: 1.99 ± 2.58 $\mu g.cm^{-2}$, saturated FAs: 1.88 ± 2.50 $\mu g \cdot cm^{-2}$, mono-unsaturated FA: 0.07 ± 0.07 $\mu g \cdot cm^{-2}$). The highest concentrations of poly-unsaturated FA were however registered in the downstream section of the GRG River (3.38 ± 4.14 $\mu g \cdot cm^{-2}$) whereas the lowest were found in the upstream section of the RPE River (0.03 ± 0.02 $\mu g \cdot cm^{-2}$).

Palmitic acid (16:0) was on average the most abundant fatty acid followed by stearic acid (18:0), palmitoleic acid (16:1n-7) and eicosapentaenoic acid (20:5n-3, Fig 2).

In downstream sites, eicosapentaenoic acid (EPA) and arachidonic acid (20:4n-6) were significantly negatively correlated with CLD concentration (respectively: r=-0.54, p=0.0268 and r=-0.51, p=0.0355). Saturated fatty acids were significantly positively correlated with CLD concentration (r=0.52, p=0.0340). All correlations between CLD and fatty acids are reported in Supp. Mat. Table 1.

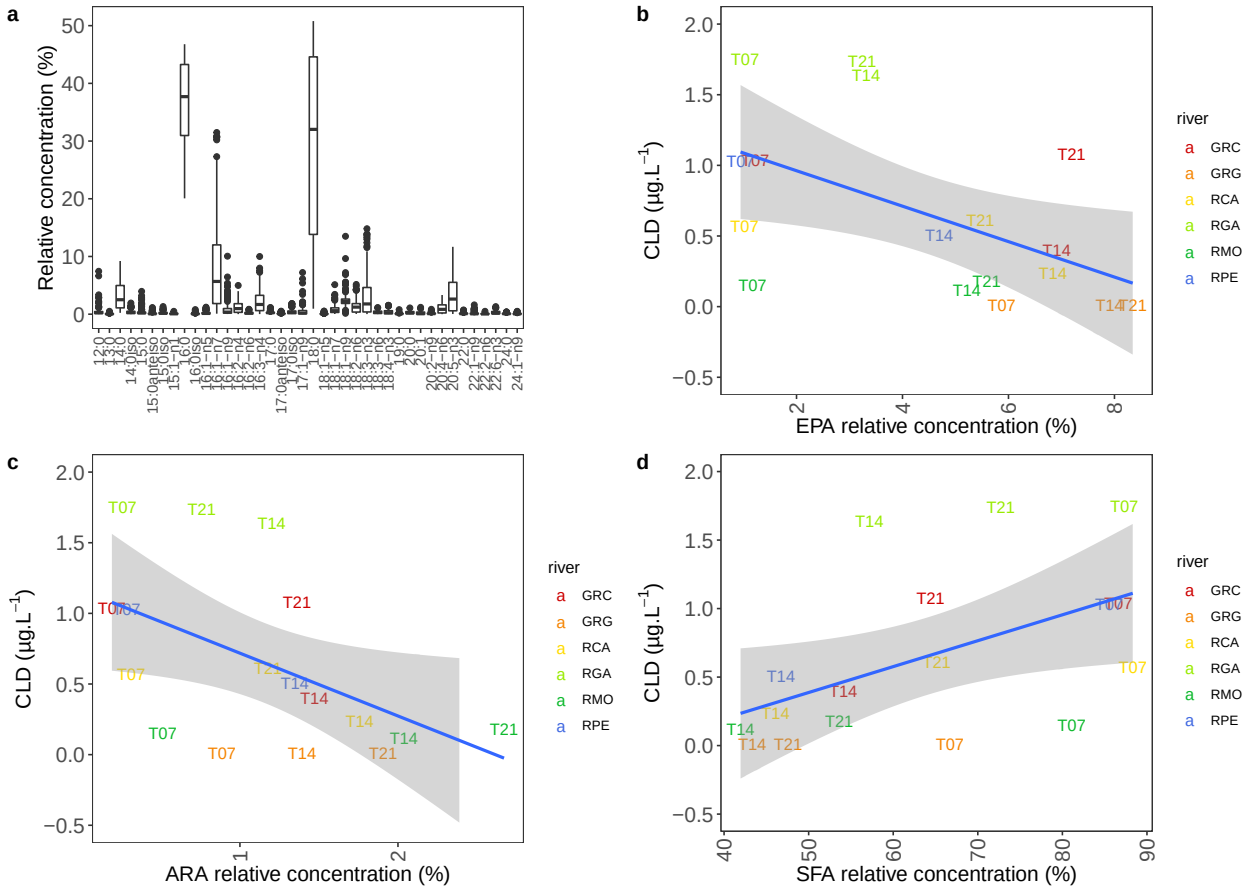

*Figure 2: **a**: Relative concentration (in %) of fatty acids at all sites, all rivers and all sampling times. **b**, **c** and **d**: Relationships between eicosapentaenoic acid (b: EPA=20:5n-3 ; F test, adjusted R^2=0.24, df1=1, df2=15, p=0.0268), arachidonic acid (c: ARA=20:4n-6 ; ; F test, adjusted R^2=0.27, df1=1, df2=15, p=0.0355) or saturated fatty acids (d: SFA ; F test, adjusted R^2=0.27, df1=1, df2=15, p=0.0340) relative concentrations and CLD concentrations in downstream sites. For each site, the sampling date is indicated (i.e. T7, T14 and T21 days after immersion of the glass slides).*

Pigment composition: The highest mean concentrations of chlorophyll *a*, chlorophyll *b*, xanthophylls and carotenes were always recorded in the downstream sites. Chlorophyll *a* was on average the most abundant pigment followed by fucoxanthin, chlorophyll *a* allomer and chlorophyll *b* (Fig 3).

In downstream sites, the proportion of fucoxanthin (a dominant and essential pigment of diatoms, Kuczynska et al., 2015) was significantly negatively correlated with the CLD concentration (r=-

0.54, df=15, p=0.02429). In addition, CLD concentration was also significantly correlated to Chlorophyll *a*, *c2* and *c3*, lutein, *p*heophytin *a* and violaxanthin (respectively r=0.63, -0.56, -0.74, -0.54, 0.61, -0.65 and 0.56, p=0.007, 0.020, 0.001, 0.010, 0.005 and 0.021). All correlations between CLD and fatty acids are reported in Supp. Mat. Table 2.

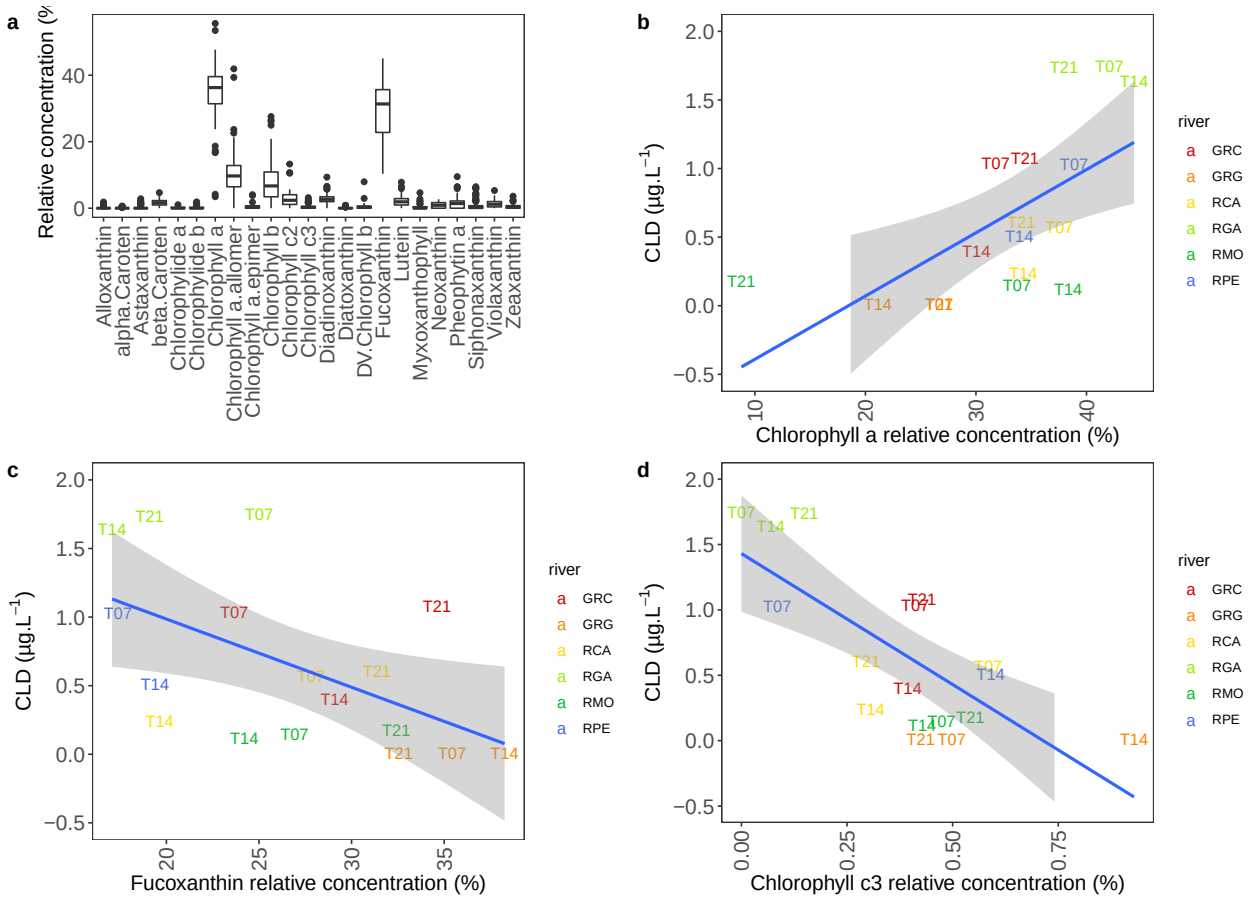

*Figure 3: **a**: Relative concentration (in %) of lipophilic pigments at all sites, all rivers and all sampling times. **b**, **c** and **d**: Relationships between chlorophyll a (b: F test, adjusted R^2=0.36, df1=1, df2=15, p=0.0067), fucoxanthin (c: F test, adjusted R^2=0.25, df1=1, df2=15, p=0.0243) or chlorophyll c3 (d: F test, adjusted R^2=0.52, df1=1, df2=15, p=0.0006) relative concentrations and CLD concentrations in downstream sites. For each site, the sampling date is indicated (i.e. T7, T14 and T21 days after immersion of the glass slides).*

EPS monosaccharide composition: On average, the highest concentrations of EPS monosaccharides were found in the downstream section of GRG and the lowest in the upstream section of GRG. Glucose was in average the most abundant sugar followed by mannose, and galactose (Fig 4).

CLD concentration was only significantly correlated to log transformed myo-inositol, scyllo-inositol and glucuronic acid (respectively r = -0.74, 0.58 and 0.56, p = 0.0007, 0.015 and 0.019). In addition it was also significantly correlated to the logarithm of the myo- to scyllo-Inositol and myo- to glucuronic acid ratio (respectively r=-0.70 and -0.59, p=0.002 and 0.014) (Fig. 4). These ratios

were also significantly higher in the downstream sites than in the upstream sites (permutation Welch *t* test, p=0.002, Fig. 4). All correlations between CLD and monosaccharides are reported in Supp. Mat. Table 3.

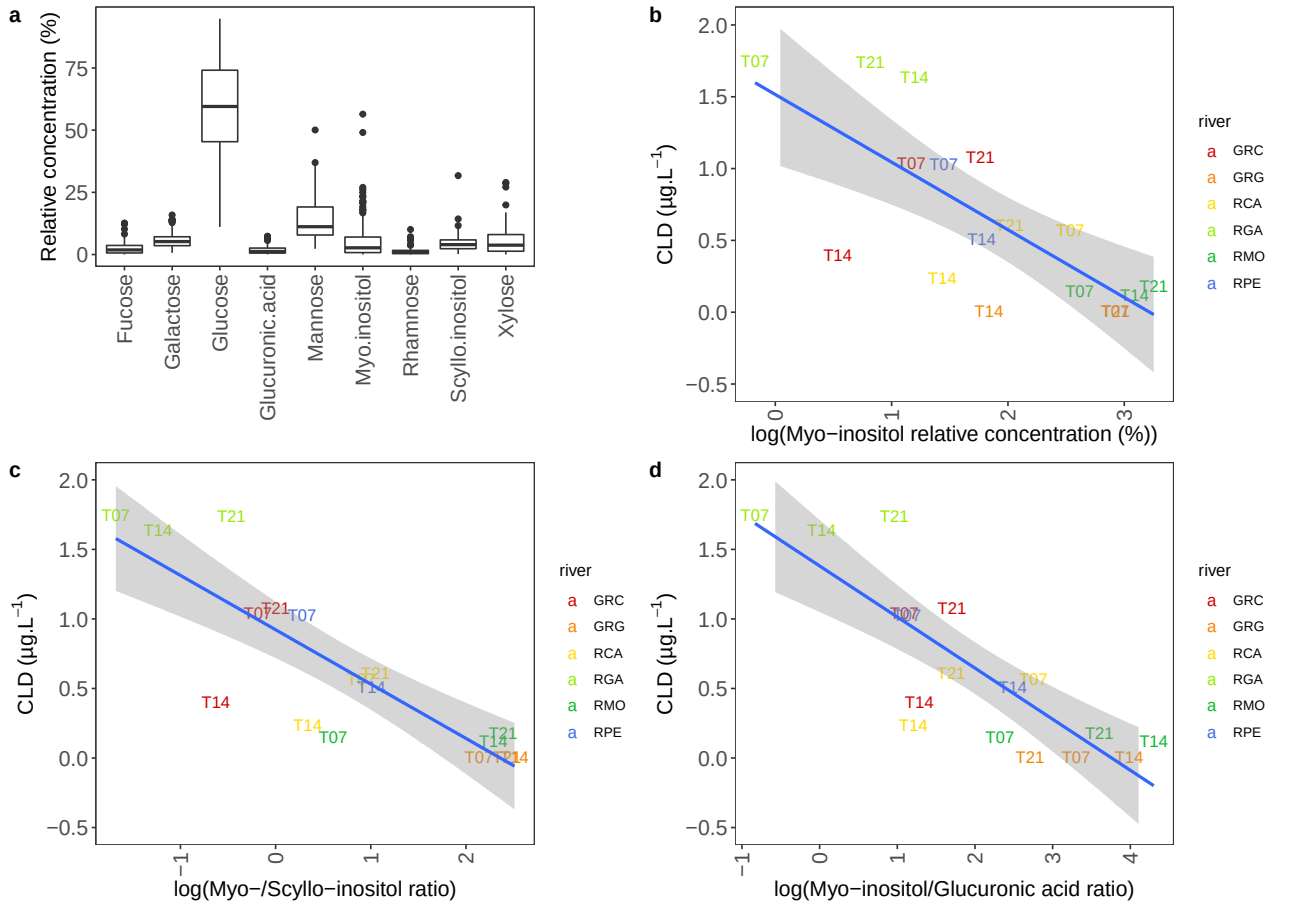

*Figure 4: **a**: Relative concentration (in %) of monosaccharides at all sites, all rivers and all sampling times. **b**, **c** and **d**: Relationships between log transformed myo-inositol percentage (b: F test, adjusted R^2=0.52, df1=1, df2=15, p=0.0007), myo- to scyllo-Inositol ratio (c: F test, adjusted R^2=0.68, df1=1, df2=15, p<0.0001) or myo-Inositol to glucuronic acid ratio (d: F tests, adjusted R^2=0.66, df1=1, df2=15, p<0.0001) and CLD concentrations in downstream sites. For each site, the sampling date is indicated (i.e. T7, T14 and T21 days after immersion of the glass slides).*

Combination of biochemical fingerprints: The two first axes of the MFA analysis (Fig. 5a) explained 47% of the total inertia. Pigments contributions to axis 1 and 2 were respectively 37 and 17%, monosaccharides contributions were 38 and 9%, fatty acids contributions were 25 and 75%. The first axis separated the different sites and represented an axis of CLD pollution (Pearson correlation between MFA axis 1 and CLD concentrations: r=0.62, p=0.0080).

By decreasing order, the main variables displaying a contribution higher than the bulk average contribution were: Scyllo-inositol, Mannose, Glucuronic acid, Xylose, Fucose, Glucose,

Chlorophyll *c3*, Fucoxanthin, Chlorophyll *c2*, Lutein, Rhamnose, Neoxanthin, Galactose, Diadinoxanthin, Chlorophyll *a*, Violaxanthin, β-β caroten, Phaeophytin *a*, β-ε caroten, Diatoxanthin, 18:1n-9, 12.0, Chlorophyll *b*, 17:0anteiso, 22:1n-9 and 17:0. These variables explained 79% of the inertia of axis1. The main variables explaining most axis2 inertia (83%) were: 16:2n-6, 14:0iso, 16:0, 20:4n-6, 18:1n-7, 18:0, Galactose, 16:0iso, 18:2n-6, 15:1n-1, β-ε caroten, 18:1n-5, 22:2n-6, 15:0iso, 17:0iso, 14:0, 16:1n-5, 15:0anteiso, 18:3n-3, 20:0, Myo-inositol, Phaeophytin *a*, Astaxanthin, 16:3n-4, 19:0, 16:1n-9, 16:2n-4, Alloxanthin, Glucose, 20:5n-3, 15:0, 18:4n-3, Chlorophyll *a*, 17:1n-9.

Our results showed that FA, pigments, EPS monosaccharides were significantly different between sites and across time (Permanova p=0.001 for site and time effect and interaction).

The BC-MFA performed using CLD pollution context as an instrumental variable (Fig.5b) showed that CLD was clearly distributed along axis 1 (Pearson correlation between BC-MFA axis 1 and CLD concentrations: $r=0.81$, $p<0.0001$) and explained 21% of total inertia of the whole biochemical dataset (Monte-Carlo test based on 999 replicates, p=0.016). The most important variables in explaining CLD categories were fucoxanthin, diadinoxanthin and lutein (for pigments, with respectively a correlation coefficient with axis 1: r = 0.64, 0.63 and -0.63), myo-inositol, scyllo-inositol and glucuronic acid (for monosaccharides, with r = 0.56, -0.56 and 0.50) and 16:2n-4, 16:1n-7 and 16:3n-4 (for fatty acids, with r = 0.70, 0.68 and 0.63).

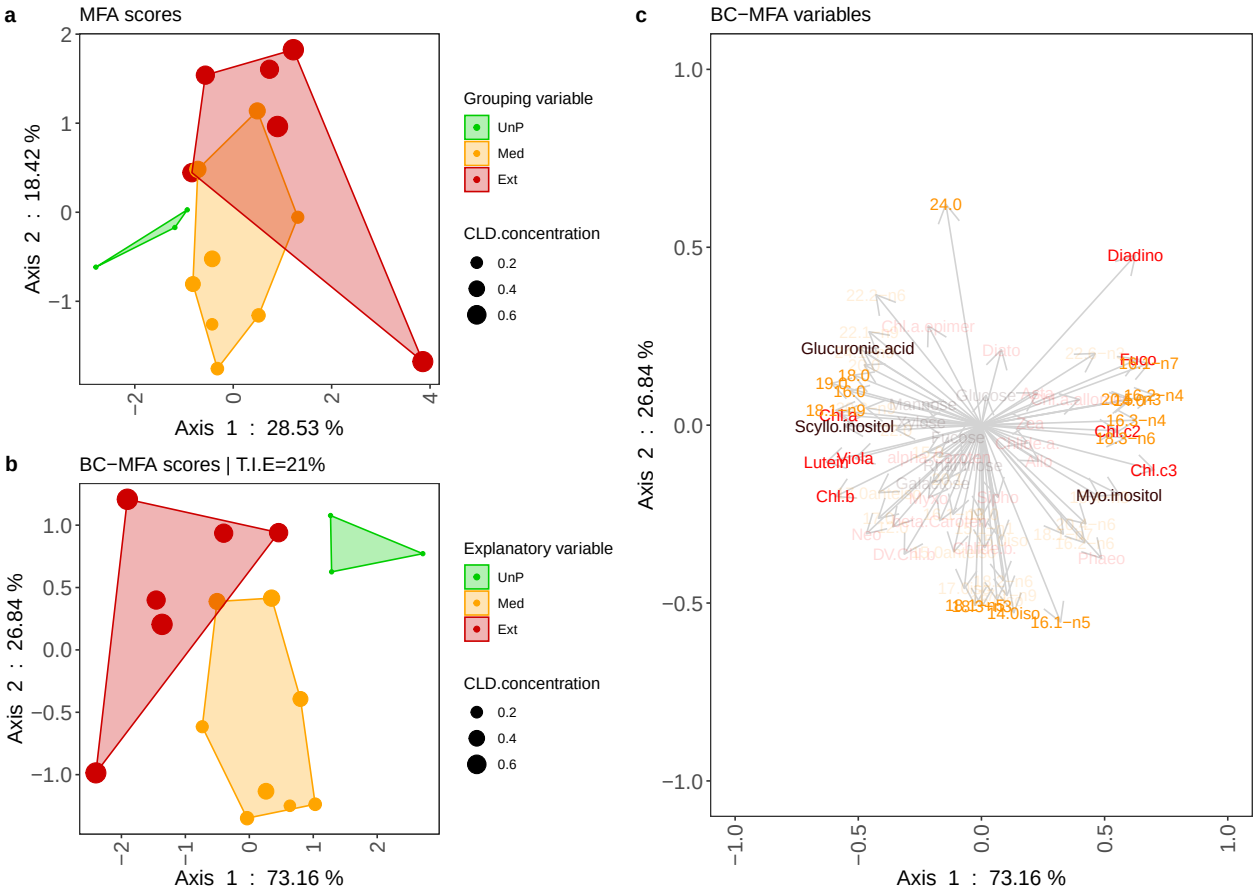

Figure 5: Results of the BC-MFA procedure using pigments, fatty acids and EPS monosaccharides of epilithic biofilms of the downstream sites. UnP = Unpolluted context (<0.1 µg.L^{-1}), Med = Medium pollution (from 0.1 to 1 µg.L^{-1}) and Ext = extreme pollution context (<1 µg.L^{-1}) according to Monti et al., (2020) ***a****: Multiple Factor Analysis scores using CLD pollution context as a grouping variable.* ***b****: Interclass analysis based on the results of the MFA and using the CLD pollution context as an explanatory variable (i.e. BC-MFA). Total Inertial Explained (T.I.E) by the explanatory variable was 21% (Monte-Carlo test based on 999 replicates, p=0.016). For both MFA and BC-MFA scores, points are proportional to the CLD concentration values (in µg.L^{-1})* ***c****: coordinates of the variables according to the BC-MFA ordination. A cos² threshold of 0.25 was applied to highlight the most important variables in the construction of the BC-MFA axes.*

Molecular fingerprinting of epilithic biofilms:

The MFA, based on T-RFLP fingerprints explained 26% of the total inertia. Archaea contributions to axis 1 and 2 were respectively 34 and 28%, Bacteria contributions were 31% and 47%, Eukarya contributions were 35% and 25% (Fig. 6a). Axis 1 and 2 did not allow a separation of the different sites according to the pollution contexts (Pearson correlation between MFA axis 1 and CLD concentrations: r=0.12, p=0.6386). However, our results showed that T-RFLP fingerprints were significantly different between sites and time (Permanova p=0.001 for site and time effect and interaction).

When using CLD category as an instrumental variable (Fig.6b), CLD was clearly distributed along axis 1 of the BC-MFA (Pearson correlation between BC-MFA axis 1 and CLD concentrations: r=0.62, p=0.0056) and explained 14% of total inertia of the whole molecular dataset (Monte-Carlo test based on 999 replicates, p=0.044).

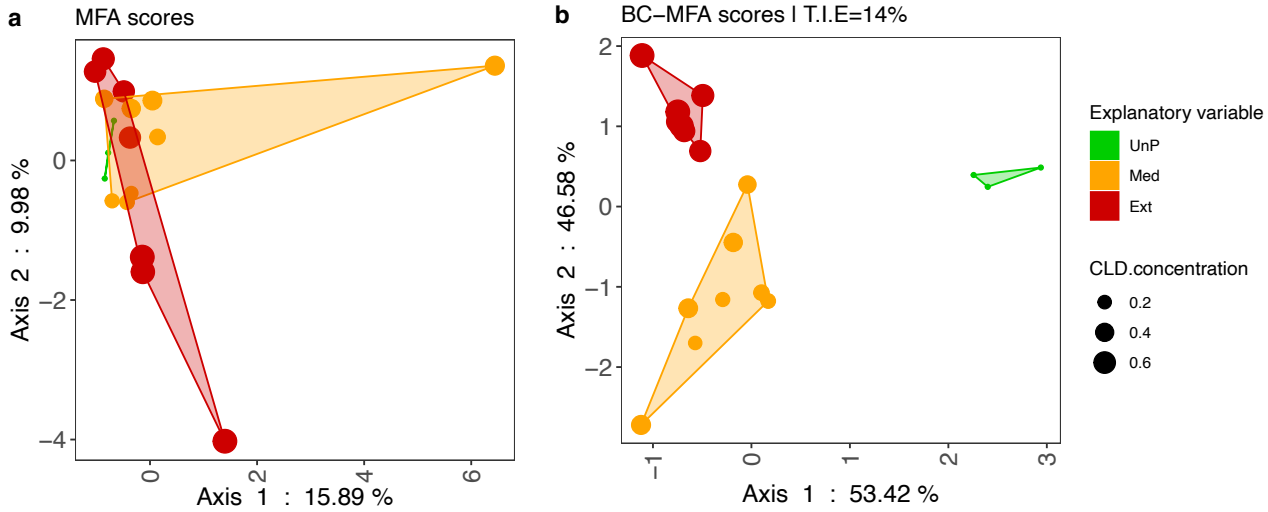

Figure 6: Results of the BC-MFA procedure using T-RFLP data of the downstream sites. UnP = Unpolluted context (<0.1 µg·L^{-1}), Med = Medium pollution (from 0.1 to 1 µg·L^{-1}) and Ext = extreme pollution context (<1 µg·L^{-1}) after Monti et al., (2020) ***a****: Multiple Factor Analysis scores using CLD pollution context as a grouping variable.* ***b****: Interclass analysis based on the results of the MFA and using the CLD pollution context as an explanatory variable (i.e. BC-MFA). Total Inertial Explained (T.I.E) by the explanatory variable was 14% (Monte-Carlo test based on 999 replicates, p=0.044). For both MFA and BC-MFA scores, points are proportional to the CLD concentration values (in µg·L^{-1}).*

Discussion

<u>CLD pollution and general context of the study:</u>

CLD concentrations in river water were highly variable between the sampling sites but were in agreement with the mapping of the potential CLD pollution risk (Fig. 1). Indeed, the most impacted rivers were in the southern part of the island where the use of the CLD was the greatest, representing a “severe” risk of contamination as reported by the French DAAF (Cabidoche et al., 2006). Our results confirmed that upstream sites were not impacted by the CLD pollution except for the RMO River.

It is unclear, however, why the upstream site of this river displayed CLD contamination levels similar to the downstream site. In a previous study, this site also showed inconsistent EPS and CLD concentration values (compared to other upstream sites), as well as viscoelastic properties that led

the authors to categorize it as "moderately polluted" a posteriori (Monti et al., 2020). Nevertheless, by focusing on the downstream sites, we showed contrasting CLD concentrations (in average RGA>RPE>GRC>RCA>RMO>GRG) in agreement with Monti et al. (2020). Multivariate analyses (Fig. 5 & 6) allowed the separation of the different downstream sampling sites according to the CLD pollution.

Microbial communities between sites were significantly different, as revealed by both chemotaxonomic and molecular fingerprints. Such differences can be explained by multiple confounding factors that could differentially influence microbial attachment and biofilm development, but this is very unlikely in the present study. Indeed, it was previously shown that the sampling sites1/ were located in water masses of similar temperature, oxygenation and pH, in identical calm facies, 2/ that they differed primarilyin the type of agricultural land use near their banks and 3/ that a meta-analysis of 2069 pesticides, obtained on the same sampling sites at the same period, confirmed the large prevalence of the CLD pollutant in the sampled rivers (Monti et al., 2020).

Changes in microbial assemblages induced by CLD pollution:

We showed that rivers characterized by contrasting CLD pollution (i.e. downstream RGA and GRG), had biofilms exhibiting different chemistry and microbial community composition. In addition, multiple factor analysis also showed that CLD pollution contexts were relatively well described by at least one axis which suggested a gradual change in epilithic biofilms in response to CLD pollution.

Biochemical fingerprints (such as fatty acids and pigments) allowed to further characterize the relationships between CLD concentration and biofilm communities. Unpolluted (UnP) rivers were marked by a higher proportion of fucoxanthin, chlorophyll *c*, and diadinoxanthin. These pigments, though not specific, are commonly used as indicators of diatoms in natural biofilms. Especially, diatoxanthin and diadinoxanthin are representative of diatom antennary complexes and, in stream periphyton, the high proportion of these pigments was related by microscopic observation to the presence of diatoms (Laviale et al., 2009). In addition, the higher contribution of several fatty acids such as 16:1n-7 and 20:5n-3, commonly used as indicators of diatoms (Dalsgaard et al., 2003; Kharlamenko et al., 1995), to UnP sites (and their co-occurrence with the above mentioned pigments within the MFA ordination) further indicates that diatoms were probably dominant within these biofilms.

Extremely polluted (Ext) sites were however characterized by a higher proportion of chlorophyll *b*, and lutein. These pigments are commonly used as indicators of Chlorophyceae and are considered

as unambiguous markers of green algae (Jeffrey, 1976; Lee, 2008). Their presence in Ext sites (and the relative absence of fucoxanthin, and diato- diadino-xanthin) indicated that the phototrophic communities were mainly dominated by Chlorophyceae. In addition, Ext biofilms were also characterized by a higher proportion of 18:1n-9, a compound commonly extracted from Chlorophyceae together with lutein and chlorophyll *b* (e.g. Wiltshire et al., 2000) but also particularly abundant in cyanobacteria (Abed et al., 2008), bacteria (Véra et al., 2001), and protozoa such as heterotrophic flagellates and amoebae (Erwin, 1973; Véra et al., 2001). Ext sites were also marked by 22:1n-9 that contributed significantly to the first axis of the MFA ordination. This fatty acid occurs naturally (but in small amounts) in animal tissues but has never been reported in significant amount in either Chlorophyceae or cyanobacteria. In mycobacterium, it was suggested that 22:1n-9 originate mainly from 18:1n-9 followed by subsequent C-2 chain elongation (Hung and Walker, 1970). Thus, 18:1n-9 and 22:1n-9 might have a bacterial origin at these sites. This was confirmed by the prevalence of saturated fatty acids (18:0, 19:0 and 16:0) and a higher proportion of 17:0 and 17:0anteiso fatty acids. These branched fatty acids are particularly abundant in bacteria and thereby commonly used as biomarkers for these groups (Kaneda, 1991).

Together, these results suggest that CLD pollution hindered diatom development and/or promoted bacterial proliferation. This is consistent with previous micro-indentation measurements showing that the CLD-polluted biofilm consisted mainly of bacteria embedded in a thin layer of low-viscosity EPS, whereas the unpolluted biofilms contained large diatoms and/or a more complex or mature EPS network with a high surface viscosity (Monti et al., 2020).

Changes in microbial EPS monosaccharides according to CLD pollution:

Microbial exopolysaccharides were further investigated by measuring EPS monosaccharide compositions of epilithic biofilms. EPS have already been associated with numerous ecosystem functions, including stabilization, food source and photosynthesis (Bellinger et al., 2009; Passarelli et al., 2015; Zhou et al., 1998). The MFA analysis revealed that the most contaminated sites (Ext sites) were characterized by a higher proportion of deoxy-sugars such as fucose and rhamnose, and pentose (xylose), which are known to promote sediment biostabilization by enhancing biofilm hydrophobicity (Zhou et al., 1998). The monosaccharide composition may depend, as well, on the ability of different bacterial groups to degrade EPS carbohydrates (Taylor et al., 2013). For instance, glucose may act as weak links, or access points, for bacterial degradation, as opposed to fucose- or rhamnose-rich exopolymers. The higher proportion of deoxy-sugar over glucose in contaminated sites may result from a higher bacterial glucosidase activity (Giroldo et al., 2003) and further confirmed the bacterial dominance at these sites.

CLD polluted biofilms EPS with increased adsorption and adhesion properties

In the present study, CLD was significantly related to EPS inositols and glucuronic acid. Monosaccharides have relatively similar numbers of CH and OH groups, and the hydration behaviour of monosaccharide is related to the orientation (i.e. equatorial vs. axial group) of the hydroxyl group (Kabayama and Patterson, 1958). Hydrogen bonds between sugar hydroxyl groups and adjacent water molecules in aqueous solution give the saccharide its hydrophobic character. Even if this is considerably weak, different monosaccharides will display contrasting hydrophobic, and therefore stabilizing and absorptive capacities (Miyajima et al., 1988).

Uronic acids, such as glucuronic acid, introduce additional carboxylate groups to the biofilm, which facilitate the fixation of cells via polyvalent metal ions (e.g. Ca^{2+}, Fe^{2+}) cross links (Bellinger et al., 2009; Poulsen et al., 2014). These charged functional groups serve as natural adsorptive and adhesive source, and provide binding sites for charged particles/molecules including several pollutants (Bhaskar and Bhosle, 2006) such as CLD. Uronic acid rich polysaccharides are major constituents of the adhesive biofilms of bacteria and several diatom species (Poulsen et al., 2014; Sutherland, 2001)

The origin of the scyllo-inositol in epilithic biofilms is unclear because stereoisomers, other than the widely distributed myo-inositol, are rare in biological tissues (L'Annunziata, 2007). Scyllo-inositol may originate from inositol phosphates, which are quantitatively important in soils. Indeed, the second most abundant inositol phosphate isomer is scyllo-inositol and has been found in large quantities in soils, sometimes exceeding myo-inositol (Turner, 2007). However, despite this widespread occurrence in soils, the scyllo-inositol (and other isomers than myo-) has been detected rarely elsewhere in nature and its origin in soil is still unknown. It has been suggested that microbes play a key role in the synthesis of this compound to protect phosphorus from uptake by nearby competing organisms, although it has never been detected in any soil organism (Turner, 2007). Also, it has been observed that amongst stereoisomeric inositol phosphates, scyllo-inositol is extremely resistant to hydrolysis in comparison to myo-inositol (Turner, 2007). This feature (i.e. active but biologically recalcitrant and hence nutritionally useless) makes it a good protection against erosion by stabilizing clay-metal-humic complexes or alternatively against pollution by forming precipitates with metals.

In our study, a causal link cannot be established between glucuronic acid or scyllo-inositol and CLD. However, the enrichment of biofilms, in polluted sites, with compounds exhibiting increased adsorption and adhesion capacities suggested that microbial assemblages might respond to CLD pollution by developing pollutant scavenging strategies.

Altogether, our results pave the way for the hitherto unsuspected role of exopolymeric substances in tropical epilithic biofilms and encourage further studies to focus on these extracellular molecules in order to develop bioindicators of pollution. For instance, simple quantitative bioassay methods for the uronic and glucuronic acid content of biofilm EPS (Mojica et al., 2007) may represent potential bioindicators for monitoring and report environmental health status in tropical freshwater ecosystems.

Author contributions

Conceptualization: D.M., C.H., R.D., B.L.;

Funding acquisition: D.M. (ANR CESA 01902), R.D., B.L. (T.R. Ph. D. grant), C.H. (SU Emergence grant)

Supervision: D.M. (PI), C.H., R.D., B.L., T.M., H.B. (WP leaders);

Project administration: D.M., B.L., C.H.;

Formal analysis: C.H., J.M.M., N.Thiney. (biochemical analyses), H.B., N. Tapie, S.A., P.D., T.R. (chemical analyses of chlordecone), A.C., T.R., S.K., B.L. (T-RFLP analyses);

Data curation: C.H.;

Writing – original draft: C.H.;

Writing – review & editing: C.H., D.M., R.D., T.M., J.M.M., B.L.;

Acknowledgements

This research was funded by grants from the Agence Nationale de la Recherche (CHLORINDIC project, ANR CESA 01902) to the coordinator D. Monti and the teams cited in the front page. B.L and R.D. benefited from a grant of the Excellence Initiative of Université de Pau et des Pays de l''Adour – I-Site E2S UPPA, a French “Investissements d''Avenir” programme. C.H. benefited from an Alliance Sorbonne Université Émergence grant (MicroBE project). The authors thank the Office de l''Eau de la Guadeloupe for the communication of their database of pesticides contamination, the French DAAF (Direction de l'Alimentation, de l'Agriculture et de la Forêt de Guadeloupe) for providing shapefiles of the potential CLD pollution, C. Barbeyron, Y. Bercion, F. Busson, S. Cordonnier, R. Kanan, C. Joubert, C. Lord-Daunay, and J.-L. Pernollet for assistance in field work, experiments, and helpful comments. We would like to thanks anonymous reviewers for their constructive comments and Taylor Smith for proofreading and checking the English.

References

Abed, R.M.M., Kohls, K., Schoon, R., Scherf, A.-K., Schacht, M., Palinska, K. a, Al-Hassani, H., Hamza, W., Rullkötter, J., Golubic, S., 2008. Lipid biomarkers, pigments and cyanobacterial diversity of microbial mats across intertidal flats of the arid coast of the Arabian Gulf (Abu Dhabi, UAE). FEMS Microbiol. Ecol. 65, 449–462. https://doi.org/10.1111/j.1574-6941.2008.00537.x

Amann, R.I., Binder, B.J., Olson, R.J., Chisholm, S.W., Devereux, R., Stahl, D.A., 1990. Combination of 16S rRNA-Targeted Oligonucleotide Probes with Flow Cytometry for Analyzing Mixed Microbial Populations. Appl. Environ. Microbiol. 56, 1919–1925.

Bellinger, B.J., Underwood, G.J.C., Ziegler, S.E., Gretz, M.R., 2009. Significance of diatom-derived polymers in carbon flow dynamics within estuarine biofilms determined through isotopic enrichment. Aquat. Microb. Ecol. 55, 169–187.

Belpomme, D., Irigaray, P., 2011. Environment as a potential key determinant of the continued increase of prostate cancer incidence in martinique. Prostate Cancer 2011, 819010. https://doi.org/10.1155/2011/819010

Bhaskar, P. V, Bhosle, N.B., 2006. Bacterial extracellular polymeric substance (EPS): A carrier of heavy metals in the marine food-chain. Environ. Int. 32, 191–198.

Bligh, E.G., Dyer, W.J., 1959. A Rapid Method of Total Lipid Extraction and Purification. Can. J. Biochem. Physiol. 37, 911–917.

Brotas, V., Plante-Cuny, M.-R., 2003. The use of HPLC pigment analysis to study microphytobenthos communities. Acta Oecologica 24, S109--S115. https://doi.org/10.1016/S1146-609X(03)00013-4

Cabidoche, Y.-M., Jannoyer, M., Vannière, H., 2006. Conclusions du Groupe d'{é}tude et de prospective. Pollution par les organochlor{é}s aux Antilles : aspects agronomiques.

Coat, S., Monti, D., Bouchon, C., Lepoint, G., 2009. Trophic relationships in a tropical stream food web assessed by stable isotope analysis. Freshw. Biol. 54, 1028–1041. https://doi.org/10.1111/j.1365-2427.2008.02149.x

Crabit, A., Cattan, P., Colin, F., Voltz, M., 2016. Soil and river contamination patterns of chlordecone in a tropical volcanic catchment in the French West Indies (Guadeloupe). Environ. Pollut. 212, 615–626. https://doi.org/10.1016/J.ENVPOL.2016.02.055

Culman, S., Bukowski, R., Gauch, H., Cadillo-Quiroz, H., Buckley, D., 2009. T-REX: software for the processing and analysis of T-RFLP data. BMC Bioinformatics 10, 171.

Dalsgaard, J., St John, M., Kattner, G., Müller-Navarra, D., Hagen, W., 2003. Fatty acid trophic markers in the pelagic marine environment. Adv. Mar. Biol. 46, 225–340.

Decho, A.W., 2000. Microbial biofilms in intertidal systems : an overview. Cont. Shelf Res. 20, 1257–1273.

Decho, A.W., Norman, R.S., Visscher, P.T., 2010. Quorum sensing in natural environments: emerging views from microbial mats. Trends Microbiol. 18, 73–80.

Dolfing, J., Novak, I., Archelas, A., Macarie, H., 2012. Gibbs Free Energy of Formation of Chlordecone and Potential Degradation Products: Implications for Remediation Strategies and Environmental Fate. Environ. Sci. {&} Technol. 46, 8131–8139.

Erwin, J., 1973. Comparative biochemistry of fatty acids in eukaryotic microorganisms, in: Erwin, Joseph (Ed.), Lipids and Biomembranes of Eukaryotic Microorganisms. Elsevier, pp. 41–143. https://doi.org/10.1016/B978-0-12-242050-4.50008-2

Escofier, B., Pagès, J., 1994. Multiple factor analysis (AFMULT package). Comput. Stat. {&} Data Anal. 18, 121–140.

Fernández-Bayo, J.D., Saison, C., Voltz, M., Disko, U., Hofmann, D., Berns, A.E., 2013. Chlordecone fate and mineralisation in a tropical soil (andosol) microcosm under aerobic conditions. Sci. Total Environ. 463–464, 395–403. https://doi.org/10.1016/j.scitotenv.2013.06.044

Frotté, L., Bec, A., Hubas, C., Perrière, F., Cordonnier, S., Bezault, E., Monti, D., 2021. Upstream/downstream food quality differences in a Caribbean Island River. Aquat. Ecol. 2021 1–7. https://doi.org/10.1007/S10452-021-09887-W

Giroldo, D., Vieira, A.A.H., Paulsen, B.S., 2003. Relative increase of deoxy sugar during microbial degradation of an extracellular polysaccharide relesed by a tropical freshwater Thalassiosira sp (Bacillariophyceae). J. Phycol. 39, 1109–1115. https://doi.org/10.1111/j.0022-3646.2003.03-006.x

Huggett, R., 1989. Kepone and the James river, in: National Research Council (Ed.), Contaminated Marine Sediments: Assessment and Remediation. The National Academies Press, Washington, DC, pp. 417–496. https://doi.org/10.17226/1412

Hung, J.G., Walker, R.W., 1970. Unsaturated Fatty Acids of Mycobacteria. Lipids 8, 720–722.

Jeffrey, S.W., 1976. A Report of Green Algal Pigments in the Central North Pacific Ocean. Mar. Biol. 37, 33–37.

Kabayama, M.A., Patterson, D., 1958. The thermodynaics of mutarotation of some sugar: II. theoretical considerations. https://doi.org/10.1139/v58-079 36, 563–573. https://doi.org/10.1139/v58-079

Kaneda, T., 1991. Iso- and Anteiso-Fatty Acids in Bacteria : Biosynthesis , Function , and Taxonomic Significance. Microbiol. Rev. 55, 288–302.

Kharlamenko, V.I., Zhukova, N. V, Khotimchenko, S. V, Svetashev, V.I., Kamenev, G.M., 1995. Fatty acids as markers of food sources in a shallow- water hydrothermal ecosystem (Kraternaya Bight, Yankich Island, Kurile Islands). Mar. Ecol. Ser. 120, 231–241.

Kuczynska, P., Jemiola-Rzeminska, M., Strzalka, K., 2015. Photosynthetic Pigments in Diatoms. Mar. Drugs 13, 5847–5881. https://doi.org/10.3390/md13095847

606 Lane, D.J. 1991. 16S/23S rRNA Sequencing. In: Stackebrandt, E. and Goodfellow, M., Eds.,
607 Nucleic Acid Techniques in Bacterial Systematic, John Wiley and Sons, New York, 115-175.

608 L'Annunziata, M.F., 2007. Origins and Biochemical Transformations of Inositol Stereoisomers and
609 Their Phosphorylated Derivatives in Soils, in: Turner, B.L., Richardson, A.E., Mullaney, E.J.
610 (Eds.), Inositol Phosphates: Linking Agriculture and the Environment. CAB international, pp.
611 41–60.

612 Lavergne, C., Hugoni, M., Hubas, C., Debroas, D., Dupuy, C., Agogué, H., 2017. Diel Rhythm
613 Does Not Shape the Vertical Distribution of Bacterial and Archaeal 16S rRNA Transcript
614 Diversity in Intertidal Sediments: a Mesocosm Study. Microb. Ecol.
615 https://doi.org/10.1007/s00248-017-1048-1

616 Laviale, M., Prygiel, J., Lemoine, Y., Courseaux, A., Créach, A., 2009. Stream Periphyton
617 Photoacclimation Response in Field Conditions: Effect of Community Development and
618 Seasonal Changes. J. Phycol. 45, 1072–1082. https://doi.org/10.1111/j.1529-
619 8817.2009.00747.x

620 Lee, R.E., 2008. Phycology. Cambridge University Press, Cambridge.

621 Lefrançois, E., Coat, S., Lepoint, G., Vachiéry, N., Gros, O., Monti, D., 2011. Epilithic biofilm as a
622 key factor for small-scale river fisheries on Caribbean islands. Fish. Manag. Ecol. 18, 211–220.
623 https://doi.org/10.1111/j.1365-2400.2010.00767.x

624 Martin-laurent, F., Sahnoun, M.M., Merlin, C., Vollmer, G., Lübke, M., 2013. Detection and
625 quantification of chlordecone in contaminated soils from the French West Indies by GC-MS
626 using the 13C10-chlordecone stable isotope as a tracer. Environ. Sci. Pollut. Res.
627 10.1007/s11356--013--1839--y. https://doi.org/10.1007/s11356-013-1839-y

628 Mercier, A., Dictor, M., Harris-Hellal, J., Breeze, D., Mouvet, C., 2013. Distinct bacterial
629 community structure of 3 tropical volcanic soils from banana plantations contaminated with
630 chlordecone in Guadeloupe (French West Indies). Chemosphere 92, 787–794.
631 https://doi.org/10.1016/j.chemosphere.2013.04.016

632 Merlin, C., 2015. Recherche de la signature biologique de la dégradation du chlordécone dans le sol
633 des Antilles françaises. Université de Bourgogne.

634 Miyajima, K., Machida, K., Taga, T., Komatsu, H., Nakagaki, M., 1988. Correlation between the
635 hydrophobic nature of monosaccharides and cholates, and their hydrophobic indices. J. Chem.
636 Soc. Faraday Trans. 1 Phys. Chem. Condens. Phases 84, 2537–2544.
637 https://doi.org/10.1039/F19888402537

638 Mojica, K., Elsey, D., Cooney, M., 2007. Quantitative analysis of biofilm EPS uronic acid content.
639 J. Microbiol. Methods 71, 61–65. https://doi.org/10.1016/J.MIMET.2007.07.010

640 Monti, D., Hubas, C., Lourenço, X., Begarin, F., Haouisée, A., Romana, L., Lefrançois, E., Jestin,
641 A., Budzinski, H., Tapie, N., Risser, T., Mansot, J.-L., Keith, P., Gros, O., Lopez, P.-J., Lauga,
642 B., 2020. Physical properties of epilithic river biofilm as a new lead to perform pollution
643 bioassessments in overseas territories. Sci. Rep. 10. https://doi.org/10.1038/s41598-020-
644 73948-7

Multigner, L., Ndong, J.R., Giusti, A., Romana, M., Delacroix-Maillard, H., Cordier, S., Jégou, B., Thome, J.P., Blanchet, P., 2010. Chlordecone exposure and risk of prostate cancer. J. Clin. Oncol. 28, 3457–3462. https://doi.org/10.1200/JCO.2009.27.2153

Orndorff, S.A., Colwell, R.R., 1980. Distribution and characterization of kepone-resistant bacteria in the aquatic environment. Appl. Environ. Microbiol. 39, 611–622. https://doi.org/10.1128/AEM.39.3.611-622.1980

Passarelli, C., Meziane, T., Thiney, N., Boeuf, D., Jesus, B., Ruivo, M., Jeanthon, C., Hubas, C., 2015. Seasonal variations of the composition of microbial biofilms in sandy tidal flats: Focus of fatty acids, pigments and exopolymers. Estuar. Coast. Shelf Sci. 153, 29–37. https://doi.org/10.1016/j.ecss.2014.11.013

Poulsen, N., Kröger, N., Harrington, M.J., Brunner, E., Paasch, S., Buhmann, M.T., 2014. Isolation and biochemical characterization of underwater adhesives from diatoms. Biofouling 30, 513–523. https://doi.org/10.1080/08927014.2014.895895

Reuber, M.D., 1978. Carcinogenicity of Kepone. J. Toxicol. Envirnmental Heal. 4, 895–911.

Sogin, M.L., Gunderson, J.H., 1987. Structural Diversity of Eukaryotic Small Subunit Ribosomal RNAs Evolutionary Implications. Ann. New York Acad. Sci. 503, 125–139.

Sutherland, I., 2001. Biofilm exopolysaccharides: a strong and sticky framework. Microbiology 147, 3–9.

Takai, K., Horihoshi, K., 2000. Rapid Detection and Quantification of Members of the Archaeal Community by Quantitative PCR Using Fluorogenic Probes. Appl. Environ. Microbiol. 66, 5066–5072.

Taylor, J.D., Mckew, B.A., Kuhl, A., Mcgenity, T.J., Underwood, G.J.C., 2013. Microphytobenthic extracellular polymeric substances (EPS) in intertidal sediments fuel both generalist and specialist EPS-degrading bacteria. Limnol. Oceanogr. 58, 1463–1480. https://doi.org/10.4319/lo.2013.58.4.1463

Teske, A., Wawer, C., Muyzer, G., Ramsing, N. B. 1996. Distribution of sulfate-reducing bacteria in a stratified fjord (Mariager Fjord, Denmark) as evaluated by most-probable-number counts and denaturing gradient gel electrophoresis of PCR-amplified ribosomal DNA fragments. Applied and Environmental Microbiology, 62:1405-1415. https://doi.org/10.1128/aem.62.4.1405-1415.1996

Turner, B.L., 2007. Inositol phosphates: linking agriculture and the environment, in: Turner, B.L., Richardson, A.E., Mullaney, E.J. (Eds.), Inositol Phosphates: Linking Agriculture and the Environment. CAB international. https://doi.org/10.1079/9781845931520.0186

Véra, A., Desvilettes, C., Bec, A., Bourdier, G., 2001. Fatty acid composition of freshwater heterotrophic flagellates: an experimental study. Aquat. Microb. Ecol. 25, 271–279. https://doi.org/10.3354/ame025271

Volant, A., Bruneel, O., Desoeuvre, A., Héry, M., Casiot, C., Bru, N., Delpoux, S., Fahy, A., Javerliat, F., Bouchez, O., Duran, R., Bertin, P.N., Elbaz-Poulichet, F., Lauga, B., 2014. Diversity and spatiotemporal dynamics of bacterial communities: physicochemical and other

drivers along an acid mine drainage. FEMS Microbiol Ecol 90, 247–263. https://doi.org/10.1111/1574-6941.12394

Wei, T., Simko, V., 2021. R package “corrplot”: Visualization of a Correlation Matrix.

Wickham, H., 2016. ggplot2: Elegant Graphics for Data Analysis. Springer-Verlag, New York.

Wickham, H., Seidel, D., 2020. scales: Scale Functions for Visualization.

Wilke, C.O., 2019. cowplot: Streamlined Plot Theme and Plot Annotations for ggplot2.

Wiltshire, K.H., Boersma, M., Möller, A., Buhtz, H., 2000. Extraction of pigments and fatty acids from the green alga Scenedesmus obliquus (Chlorophyceae). Aquat. Ecol. 34, 119–126.

Zhou, J., Mopper, K., Passow, U., 1998. The role of surface-active carbohydrates in the formation of transparent exopolymer particles by bubble adsorption of seawater. Limnol. Oceanogr. 43, 1860–1871.

Supp. Material

Table 1: Correlations between CLD and fatty acids

Fatty acids	Pearson coefficient	P-value
12.0	0.27	0.3014
13.0	-0.06	0.8221
14.0	-0.46	0.0640
14.0iso	-0.26	0.3086
15.0	0.28	0.2790
15.0anteiso	0.01	0.9814
15.0iso	-0.20	0.4382
15:1-n1	-0.02	0.9282
16.0	0.51	0.0382
16.0iso	-0.22	0.3984
16:1-n5	-0.51	0.0372
16:1-n7	-0.53	0.0277
16:1-n9	0.11	0.6711
16:2-n4	-0.63	0.0071
16:2-n6	-0.52	0.0307
16:3-n4	-0.58	0.0145
17.0	0.32	0.2078
17.0anteiso	0.43	0.0815
17.0iso	-0.06	0.8309
17:1-n9	-0.34	0.1752
18.0	0.49	0.0435
18:1-n5	-0.14	0.5990
18:1-n7	-0.40	0.1073
18:1-n9	0.68	0.0027
18:2-n6	-0.26	0.3102
18:3-n3	-0.17	0.5033
18:3-n6	-0.55	0.0223
18:4-n3	-0.54	0.0253

19.0	0.56	0.0188
20.0	0.44	0.0786
20.1	0.12	0.6415
20:2-n9	0.53	0.0285
20:4-n6	-0.51	0.0355
20:5-n3	-0.54	0.0268
22.0	0.29	0.2646
22:1-n9	0.71	0.0015
22:2-n6	0.61	0.0088
22:6-n3	-0.28	0.2721
24.0	0.44	0.0761
24:1-n9	0.59	0.0125
Saturated FA	0.52	0.0340

699
700

701 Table 2: Correlations between CLD and pigments

Pigments	Pearson coefficient	P-value
Alloxanthin	-0.30	0.2455
alpha.Caroten	0.16	0.5512
Asta	-0.14	0.6044
beta.Caroten	0.21	0.4223
Chl.a	0.63	0.0067
Chl.a.allomer	-0.41	0.0999
Chl.a.epimer	0.31	0.2214
Chl.b	0.43	0.0814
Chl.c2	-0.56	0.0195
Chl.c3	-0.74	0.0006
Chlide.a.	-0.28	0.2712
Chlide.b.	-0.15	0.5653
Diadino	-0.46	0.0619
Diato	-0.20	0.4449
DV.Chl.b	0.05	0.8369
Fuco	-0.54	0.0243
Lutein	0.61	0.0096
Myxo	0.23	0.3775
Neo	0.37	0.1383
Sipho	-0.11	0.6821
Phaeo	-0.65	0.0050
Viola	0.56	0.0206
Zea	-0.22	0.3928

702
703

704 Table 3: Correlations between CLD and the logarithm of monosaccharides

Monosaccharides	Pearson coefficient	P-value
Glucuronic.acid	0.56	0.0185
Fucose	0.17	0.5058
Galactose	0.16	0.5490
Mannose	0.31	0.2318
Myo.inositol	-0.74	0.0007
Rhamnose	0.12	0.6388

Scyllo.inositol	0.58	0.0150
Xylose	0.30	0.2371
Glucose	-0.07	0.7834

705
706